An Addressable Microfluidics device for Noninvasive Manipulation of Cells and Chemicals within Live Cultures

Anh Tong,[1] Quang Long Pham,[1] Vatsal Shah,[2,3] Akshay Naik,[4] Paul Abatemarco,[1] and Roman Voronov[1,†]

[1]Otto H. York Department of Chemical and Materials Engineering, New Jersey Institute of Technology, Newark, NJ, USA

[2]Ying Wu College of Computing Sciences, Department of Computer Science, New Jersey Institute of Technology, Newark, NJ 07102, USA

[3]Federated Department of Mechanical and Industrial Engineering, New Jersey Institute of Technology, Newark, NJ 07102, USA

[4]Helen and John C. Hartmann Department of Electrical and Computer Engineering, New Jersey Institute of Technology, Newark, NJ 07102, USA

[†]Address correspondence to Prof. Roman S. Voronov, Otto H. York Department of Chemical and Materials Engineering, New Jersey Institute of Technology, Newark, NJ 07102, USA. Electronic mail: *rvoronov@njit.edu*, Fax: +1 973 596 8436, Tel: +1 973 642 4762

ABSTRACT

According to the U.S. Department of Health & Human Services, nearly 115,000 people in the U.S needed a lifesaving organ transplant in 2018, while only ~10% of them have received it. Yet, almost no artificial FDA-approved products[1] are commercially available today – three decades after the inception of tissue engineering. It is hypothesized that the major bottlenecks restricting its progress stem from lack of access to the inner pore space of the scaffolds. Specifically, the inability to deliver nutrients to, and clear waste from, the center of the scaffolds limits the size of the products that can be cultured. Likewise, the inability to monitor, and control, the cells after seeding them into the scaffold results in nonviable tissue, with an unacceptable product variability. To resolve these bottlenecks, we present a prototype addressable microfluidics device capable of non-invasive fluid and cell manipulation within living cell cultures. As proof-of-concept, we demonstrate its ability to perform additive manufacturing by seeding cells in patterns (including co-culturing multiple cell types); and subtractive manufacturing, by removing surface adherent cells via targeted trypsin release. Additionally, we show that the device is capable of sampling fluids non-invasively, from any location within the cell culturing chamber. Finally, the on-chip plumbing is completely automated using external electronics. This opens up the possibility to perform long-term computer-driven tissue engineering experiments, where the cell behavior is modulated in response to the non-invasive observations throughout the whole duration of the cultures. It is expected that the proof-of-concept technology will eventually be scaled up to 3D addressable microfluidic scaffolds, capable of overcoming the limitations bottlenecking the transition of tissue engineering technologies to the clinical setting.

INSIGHT, INNOVATION, INTEGRATION

.

INTRODUCTION

According to the U.S. Department of Health & Human Services, nearly 115,000 people in the U.S needed a lifesaving organ transplant in 2018, while only ~10% of them have received it. Yet, almost no artificial FDA-approved products[1] are commercially available today – three decades after the inception[2] of tissue engineering. The two major bottlenecks restricting the progress of recreating complex organs and tissues in vitro are: 1) product size limitation, due to inability to deliver nutrients to inner pore space of large scaffolds; and 2) product variability, due to the lack of access and control over cells post seeding.

Furthermore, each time point analysis is typically sacrificial (e.g. chemical assay that requires crushing the cultured scaffold). This inability to monitor the scaffolds continuously slows down the scientific progress tremendously, and balloons the costs of experiments. Thus, noninvasive fluid manipulation within scaffolds would revolutionize both tissue engineering and drug testing (which is the biggest practical application of the scaffolds at this point in time).

In this study, we hypothesize that in order to overcome these obstacles, an ideal scaffold should be composed of the following elements: (1) Active pores capable of delivering nutrients, oxygen and chemical signals throughout the scaffold's pore space, (2) Transparent material for real-time microscopy observation of cell behavior and tissue development, (3) Targeted localized cell seeding/chemical delivery and/or sampling to enable tissue patterning and non-invasive monitoring at different locations within the scaffold (4) Interactive, continuous, closed-loop spatial and temporal control of the biology occurring in the scaffold throughout the whole culturing process.

We further hypothesize that these goals can be achieved by merging microfluidic and scaffold technologies. Interestingly, microfluidics technologies share many characteristics with conventional biomanufacturing techniques, while at the same time lacking their major bottlenecks (see Table 1). Namely, they have the ability to seed cells with precision, perform localized chemical analysis, and are transparent to microscopic observation. Moreover, microfluidics substrates can be fabricated with even more precision than their bioprinted counterparts, but without the danger of damaging cells in the process (since they can be flown in post fabrication). And most importantly, they provide an active "vasculature" of micro-channels, which not only allow for continuous nutrient delivery and waste removal (thereby resolving product size-limitation of conventional methods), but also open up the possibility for manipulation of single-cell behavior with control-feedback from real-time monitoring.

Table 1. Comparison of existing biomanufacturing technologies (rows 2-4) with the proposed microfluidics approach (bottom row). Yellow color highlights key advantages, while Red highlights major limitations.

Tech Type	Material	Geometry	Cell Seeding	Cell Viability	Synthetic Vasculature	Culture Analysis	Culture Controls
Artificial Scaffold	Any	Poor to Precise	Random	Excellent	Passive	Bulk	Bulk
De-cellularized Organ	Natural	Natural	Random	Excellent	Passive	Bulk	Bulk
Bio-printing	Very-Limited	Precise	Precise	Poor	Passive	Bulk	Bulk
Microfluidics	Less-Limited	Precise	Precise	Excellent	Active	Localized	Localized

Therefore, the microfluidics technologies provide numerous advantages over the conventional tissue engineering approaches, so it is logical to integrate them into the scaffolds. To that end, several such attempts have been made in the past.[3-9] However, they mostly focused on developing the materials and the fabrication techniques for manufacturing of the microfluidic scaffolds, while the plumbing needed for targeted fluid and cell manipulation within them has not been designed. Specifically, it desirable to be

able to deliver / sample fluids at specified locations within the scaffold, in order to pattern the tissue and monitor its development noninvasively. However, the inclusion of dedicated channels for every such location (from here on referred to as "addresses") is inefficient, when it comes to scaling up the design to organ-sized tissues.

The problem is illustrated using a 2D example in Figure 1-LEFT. Here it is shown that for a 3x3 grid of addresses, the design suffers from: a) Poor scaling – the number of flow channels required to actuate each individual address in the grid scales as X*Y, which is the worst case scenario; and b) Resolution limitations, because the spacing available for the channels is limited by the separation distance between the addresses (which should be small, given that ideally the device should have single cell resolution). Fortunately, an old concept in the microfluidics field solves this problem by including orthogonally-blocking channels, shown in blue in Figure 1-RIGHT. By using this combination of flow and blocking (i.e., valve actuating) channels, (X+Y) scaling is achieved (i.e., only 3 flow + 3 blocking channels are required, as opposed to a total of 9 dedicated flow channels in the X*Y scaling); and the resolution is no longer limited by the crowding.

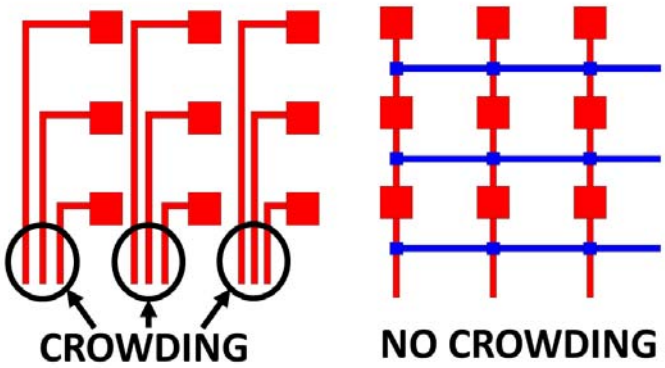

Figure 1 Difference in scalability and resolution of addressable microfluidics arrays, illustrated using a 3 x 3 grid example: LEFT – Inefficient X*Y scaling, and resolution limitations due to crowding of the supply channels; RIGHT – Efficient (X+Y) scaling, and resolution is not limited by crowding. Red = flow channels through which cells or chemicals are delivered and/or sampled; Blue = blocking (i.e., valve actuating) channels.

"Addressable" microfluidic technologies, such as in Figure 1-RIGHT have been used before for creating: an array of cell culturing chambers for high-throughput drug testing,[10] a droplet-based device for multi-parameter analysis of single microbes and microbial communities,[11] and a stencil for protein and cell patterning of substrates.[12] However, here we are interested in addressable fluid manipulation within a *single* cell culture (as opposed to each address corresponding to an isolated chamber), which has not been done before. Furthermore, we want the device to be automated, in order to enable computers to perform the manipulations over long-time culturing experiments. For the latter, we employ a modification of a programmable pneumatic technology, developed for operation and automated control of single- and multi-layer microfluidic devices.[13-15] To that end, the remainder of the manuscript presents our proof-of-concept platform, which adapts the addressable microfluidic plumbing and automation, in order to perform the noninvasive cell and chemical manipulations needed to revolutionize tissue engineering scaffolds.

METHODS

Multilayered PDMS devices were fabricated using soft photolithography. The microfluidic plumbing was actuated pneumatically via external solenoids, driven by a Wago 750 PLC controller programmed with a custom Matlab code. Directed migration of mouse embryo NIH/3T3 fibroblasts and normal human dermal fibroblasts was induced via a timed release of the platelet-derived growth factor – BB (PDGF-BB) chemoattractant. Cytoskeleton-altering drugs (Blebbistatin, cytochalasin D, and Nocodazole) and osteogenic differentiation factors (dexamethasone, b-glycerophosphate, 1,25-Dihydroxyvitamin D3, ascorbate and BMPs) were used for patterning the morphology and the lineage of human mesenchymal stem cells, respectively. A non-invasive alizarin red assay was performed by sampling the patterned culture by reversing the flow through the selected microfluidic ports. Time-lapse phase-contrast imaging of the cells behaviors were performed using a fully automated Olympus IX83 microscope operated by custom-written software.

Materials

Polydimethylsiloxane (PDMS) Sylgard 184 was purchased from Dow Corning (Midland, MI). Negative photoresist SU-8 was purchased from Microchem (Newton, MA). Positive photoresist AZ® P4620 was purchased from Integrated Micro Materials (Texas, USA). Human Fibronectin (Corning®) and recombinant human platelet-derived growth factor (PDGF-BB) were purchased from VWR (Radnor, PA). Culture media was prepared from Minimum Essential Medium (MEM) (Sigma, MO) supplemented with 10% (v/v) fetal bovine serum (FBS) (VWR, Radnor, PA) and 1% (v/v) penicillin-streptomycin (10,000 U mL-1) (Thermofisher, Waltham, MA). Basal media was composed of MEM supplemented with 1% (v/v) penicillin-streptomycin. For incubation in 5% CO2 atmosphere, media was buffered by 26 mM sodium bicarbonate (Sigma, MO). CO2-independent media buffered by 20 mM HEPES (Sigma, MO) was used for the microscope stage-top experiment. Mouse NIH3T3 fibroblasts and MSCswere provided by …

Device Concept

In order to accomplish the localized cell migration control we modified a microfluidic array with a blend of two different technologies: individually addressable chambers [10] and a programmable stencil [12]. The concept of the device is shown in Figure 2. A 4x4 array of delivery “holes ports” (red circle, Figure 2.a) connects the chemical/cell payload channels to the underneath migration chamber below (Figure 2.b). The flow is controlled using an array of O-shaped pneumatic valves (blue, Figure 2.a). When the valves are in the “open” state, the delivery holes ports are supplied with the chemical/cells and when the valves are “closed”, the chemoattractant is rerouted around the chamber ports via a “bypass”. Figure 2.b shows the device cross-section which consists of 4 layers (from top to bottom): a valve layer, a thin flexible membrane, a flow layer, and a cell migration layer. The operational mechanism of the O-shape valve is demonstrated in Figure 2.b. In the “closed” state, the pressurized valve expands causing the flexible membrane to block the chemical flow to the migration layer via the addressable ports. Conversely, in the “open” state, the chemical can flow through the addressable ports, and a localized signal is delivered to the migration layer, forming chemical gradient sources directly underneath the ports. As a consequence, the cells response to the localized chemical signal (chemoattractant in chemotaxis, or drug/vaccine in drugs/vaccines/or cytotoxic testing) (Figure 2.b).

Device Fabrication

The masks for the devices were sketched using AutoCAD (Autodesk, Mill Valey, CA) and printed at 50,800 DPI on a transparency (Fineline Imaging, Colorado Springs, CO). The devices were created using replica molding technique and the master mold are fabricated from SU-8 negative photoresist using soft photolithography technique and the custom-built mask aligner, both of which are described in our prior publication.[16] The SU-8 2010 photoresist was spin-coated at 2000 rpm on a 4-in Silicon wafer, exposed to UV light, and developed to yield 20-µm-tall microfluidic channels. The internal surfaces of the

microfluidic channels were treated with Collagen Type I (150 µg ml^{-1} coating concentration) overnight (≥ 12 hours) at 4°C or incubate at least 3 hours at 37 °C.

Cell Patterning

Device Preparation

The device was autoclaved at 121 °C for 60 mins to completely cure the uncrosslinked oligomers inside the bulk PDMS, evaporate the remained solvent from curing agent, and sterilize the PDMS device prior to adhesion surface treatment and cell seeding. Subsequently, the cell culture chamber of the device was coated with fibronectin 10ug/mL and the internal surfaces of the microfluidic channels were treated with 2% BSA at 25 °C (room temperature condition) for at least 10 hrs inside the UV chamber to maintain the sterile condition of the PDMS device. In this case, 2% BSA solution was used to prevent the adhesion of the cells to the microfluidic channel's surface.

Cell Preparation

The chosen cell type were suspended in pre-warmed complete growth DMEM medium supplemented with 10% fetal bovine serum and Gentamicin at the concentration of 50µg/mL. to the cell concentration of 5 x 10^6 cells mL^{-1}. Cells were trypsinized from a T-75 cell culture flask by adding 2 mL of 1x trypsin/EDTA (0.25%, 0.2 g L−1 EDTA) for 3 min. DMEM (8 mL) was added to neutralize the trypsin/EDTA activity. The cell suspension was centrifuged at 1000 × g for 2 min. The supernatant was removed by aspiration and the cell pellet was re-suspended in DMEM. 10 mL of suspended cells was added to dispensing bottle with 4 ports that connected to the chemical payload channels of the device. The bottle is then pressurized by 5% Carbon dioxide at 6-7 psi under constant shaking motion at 210 rpm.

PUMPING AUTOMATION: This technology is a modification of open source technology published here: https://sites.google.com/site/rafaelsmicrofluidicspage/ and here: http://pubs.acs.org/doi/abs/10.1021/ac071311w

We have built a pneumatic system based on modular industrial automation components made by WAGO. The setup is based on modular industrial automation components made by WAGO. The core of the setup is an Ethernet-based programmable WAGO-I/O-SYSTEM 750 controller, and an 8-channel digital output module (WAGO OUTPUT MODULE 750-530) that allows the controller to drive 24V Festo (MH1-A-24VDC-N-HC-8V-PR-K01-QM-APBP-CX-DX) miniature pneumatic solenoid valves. The valves are connected to a custom DYI pneumatic pumping system, which deliver the chemoattractant to the addresses. In order to avoid contact between the solenoid valves and the pumped liquid, the system contains machined reservoirs that prevent water from backup into the valves.

Cell Preparation

Mouse embryo NIH/3T3 (ATCC® CRL-1658™) fibroblasts and normal human dermal fibroblasts (NHDF) (ATCC® PCS-201-012™) were purchased from ATCC (Manassas, VA). Prior to being transferred to the microfluidic device for the migration experiments, the cells were incubated in the culture media inside of T75 flasks. The flasks were kept at 37 °C and in a humidified atmosphere of 5% CO_2 in air. The culture media was changed every two days to ensure normal cell growth. Prior to the migration experiments, the cells were trypsinized from the T75 flasks and loaded into the chip. A seeding density of about 50,000 cells cm^{-2} was used. The chip was incubated at 37 °C under 5% CO_2 for 6 hours to allow for the cell-surface adhesion. Then the NIH/3T3 cells were cultured in serum-starved media (MEM supplemented with 1% penicillin-streptomycin) for 6 hours, while the NHDF culture media was

supplemented with 0.5% FBS to provide minimal survival condition for the long-term experiments (because they are slower).

Cell Migration Experiment

For full details of the experimental setup, see our previously published work.[17] Briefly, at the start of the experiment, cell culture media in the chip was replaced with CO_2-independent media (basal for NIH/3T3 or 0.5% FBS for NHDF), buffered by HEPES and supplemented with 1% penicillin-streptomycin. 20 µL of the basal media supplemented with 50 ng mL^{-1} PDGF-BB was then added into the central reservoir of each device. Typically, the device was mounted on a condition chamber which is equipped with a temperature regulation system and a humidified environment. Time-lapse phase-contrast imaging of the fibroblast migration was performed using a fully automated Olympus IX83 microscope fitted with a 10X phase-contrast objective (Olympus, Japan), a CMOS camera (Orca Flash 4.0 V2, Hamamatsu, Japan), and an autofocus module (ZDC, Olympus, Japan). Time-lapse images were automatically captured at a 27 minute interval for duration of 5-10 days (media refreshed after 5 days) for NHDF and at a 15 minute interval for a duration of 24 hours for NIH/3T3 cell. For each device at each time step, 36 tile images were acquired at different locations, stitched, and stabilized using an in-house Matlab® 2016b code (MathWorks, Inc., Natick, MA).

Data Analysis

The migrating cells were tracked using the Manual Tracking plug-in for ImageJ software (National Institutes of Health).[18] The directional decisions chosen by each individual cell at the bifurcation were determined via manual observation. Quantitative data of cell sequences was generated using an in-house Matlab® 2016b code (MathWorks, Inc., Natick, MA). Significance level was determined by using a non-parametric test for a binomial distribution, unless otherwise stated. Statistical significance was set as $p < 0.05$.

RESULTS

In this manuscript, we have realized an envisioned proof-of-concept automated microfluidic platform, capable of noninvasive XY fluid manipulation within live 2D cultures. To do this, we used a combination of micro-sized flow channels and blocking pneumatic valves, in order to actuate the individual addresses *independently* of each other. After going through multiple iterations of the plumbing design, we have converged upon the result shown in Figure 2a. There, the addressable array has a 4x4 size for simplicity, though the actual grid size is a free parameter. Each of the addresses in the array are shown as red-discs, and are surrounded by O-shaped pneumatic valves (shown as blue circles). When the valve is "*closed*" (see the inset in Figure 2a), the fluid traveling through the red channels is re-routed around the address via a thin bypass channel (also labeled in red). However, when a valve is "*open*", the corresponding address can either deliver or withdraw (depending on the direction of the flow in the red channels) the fluid carrying a chemical payload, and/or cells, to/from the culture layer below (see Figure 2b).

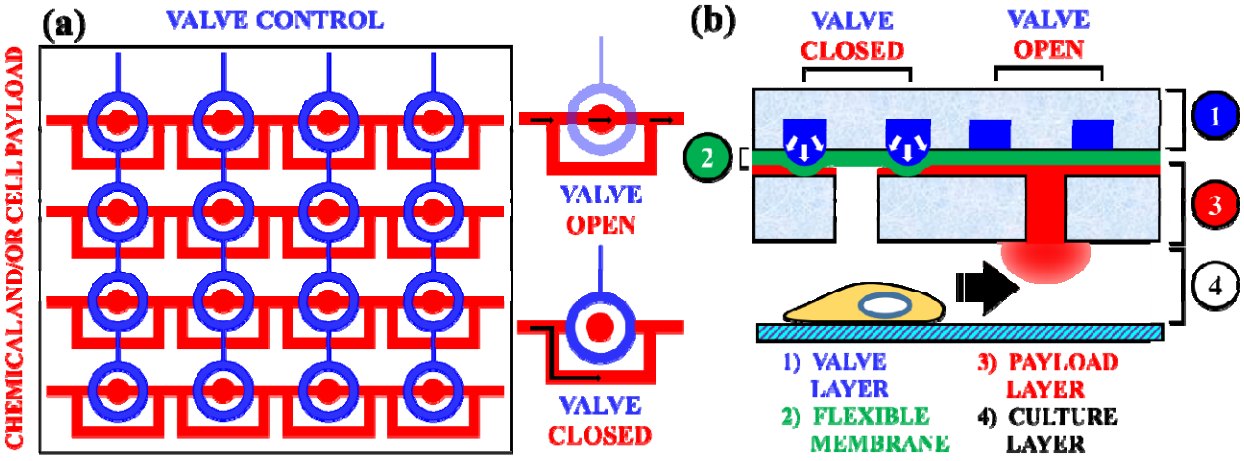

Figure 2 Schematic of the Addressable Microfluidic Plumbing. (a) Top XY view of a 4x4 matrix of "addressable" ports. Flow channels are shown in red, and blocking valve channels are in blue. Inset shows that a port is active when the valve is "open", and bypassed when it is "closed". Black arrows indicate direction of flow, which assumes payload *delivery* to (as opposed to *sampling* at) an address. (b) Z cross-section of the same device, showing how a cell neighboring an open microfluidic port is attracted towards chemical payload released through it into the 'culture layer'. At the same time, it is shown that the closed port directly above it, does not affect the cell.

Figure 2b is a Z cross-section of the device, which shows that it consists of 4 main layers (from top to bottom): a valve layer, a thin flexible membrane, a flow layer, and a cell culture layer. The action of the O-shaped valve is also shown in the same figure: in the "*closed*" state, the pressurized valve expands, causing the flexible membrane to block flow to the address; conversely, in the "*open*" state, the flow is allowed to enter the address freely, where a microfluidic port then connects it with the culture layer below. As an example, a chemical payload can be delivered through this port in order to attract a neighboring cell. At the same time, the *closed* port directly above the cell would not affect its behavior.

Some manipulations possible with the fluid manipulation within the device are: 1) Seeding different cell types in varied amounts and pre-determined patterns; 2) Nourishing them by continuously renewing the culture media, or induce migration by establishing a nutrient or a chemoattractant gradient; 3) Patterning tissue via delivery of growth and/or differentiation factors to specified locations within the device; 4) Modifying cell morphology via delivery of cytoskeleton-altering drugs to selected cells; and 5) Sampling a living culture non-invasively, by picking up and, sending off for analysis, effluents from different locations above the cells.

The action of delivering and sampling chemicals within the addressable device is shown in the left and right panes of Figure 3, respectively. In the former case, a purple dye is delivered to the right bottom corner of a 4x4 array of microfluidic ports; while in the latter case, the same purple dye is withdrawn back via a port at the opposite end of the same address row. As a possible application, the picked up fluid could be a cell culture effluent, which would then be sent off to an external sensor for non-invasive analysis. This would eliminate the reliance on destructive chemical assays, ensuring continuous monitoring of the biology occurring within live cultures. Furthermore, it can be done continuously over long period of time, given that the whole process is automated, and as such, does not require any human involvement. **Video 1** shows the operation of the device over time.

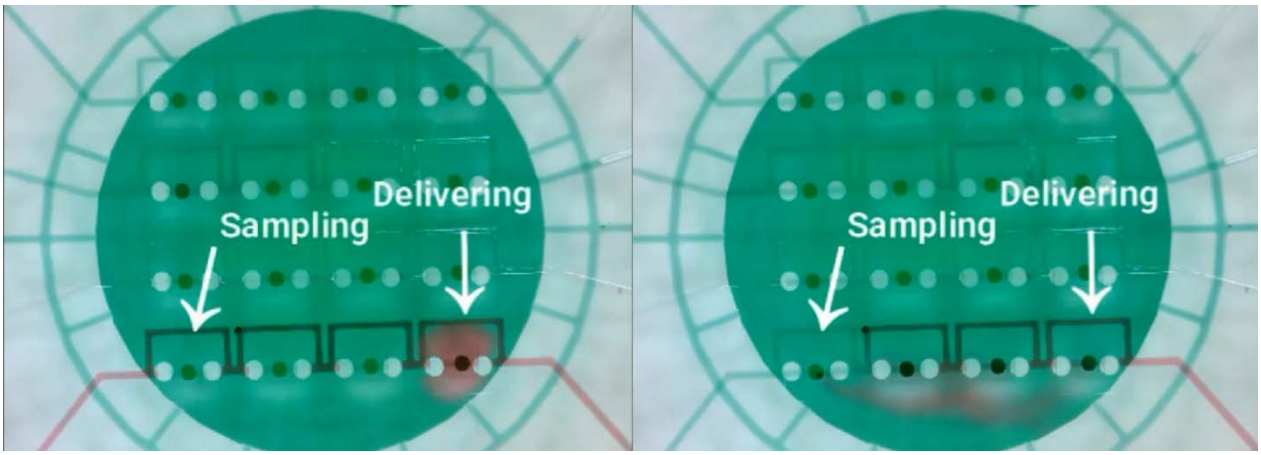

Figure 3 Microscopy of the addressable microfluidics device, showing: LEFT - delivery of a purple dye to the bottom right corner port in the 4x4 grid; RIGHT - sampling of the delivered purple dye via the bottom left corner port in the 4x4 grid. . Each port is 150 μm in diameter, and the channels are 100 μm in width.

DISCUSSION

The goal of this work was to create a technology capable of real time noninvasive observation and control of cell behavior within artificial tissues. The ability to do so would clear major bottlenecks to the advancement of organ manufacturing and drug testing using organ mimics. To that end, we hypothesized that microfluidics technologies can use addressable fluid manipulation to enable chemical delivery, and noninvasive culture effluent sampling, at targeted locations within tissue scaffolds. To that end, we have fabricated a proof-of-concept device, which is capable of performing the said operations within a 2D cell culture. Furthermore, we automated the device, in order to eliminate the reliance on human labor over the long term culturing periods, typically expected in tissue engineering.

As a result, we have shown that the device is capable of a localized payload delivery, directly below any activated address via an assembly of pneumatic valving and microfluidic ports.

A major disadvantage of the existing biomanufacturing methods is the disconnect that currently exists between tissue fabrication and its culturing. However, it is anticipated that in the near future microfluidics will merge with 3D (bio)printing. In other words, it will become possible to 3D-print tissue scaffolds interlaced with microfluidic channels (see Section D3). These channels could then be utilized for interactive tissue-assembly, yielding the much-needed resolution and improved cell viability. Moreover, this complementary "marriage" of the two technologies would blur the line between fabrication and culturing stages of the tissue-manufacturing process. Instead, it would make the whole thing *continuous*, thereby allowing to retain the precision, and the control over individual cells, into the culturing stage.

Moreover, although this proposal concentrates on migration (as a proof-of-concept study), the same approach can be readily extended to delivery / analysis of *other* cell stimuli or byproducts. Thereby, differentiation, proliferation and tissue deposition could all be controlled (not possible using existing methods). For example, in vivo organogenesis occurs in multiple-steps; this is illustrated by how most bones in our bodies start out as cartilage, and only subsequently become calcified through a process called endochondral ossification. Conversely, the state-of-the-art in-vitro tissue patterning techniques are achieved in the following ways: 1) allocating a separate nozzle per each *pre-processed* cell line (as in the case of bioprinting), 2) fabricating growth factors and morphological cues into the substrate or bio-ink, and/or 3) *post-processing* with exogenous stimuli. While the first approach is limited to a single step, the other two cannot target individual cells, nor are they responsive to cell behavior (i.e., they are open-loop).

Conversely, our approach could be used to design a platform capable of dynamic, benign tissue patterning with single-cell precision.

Finally, the ability to control cell migration could be applied in other, non-tissue engineering studies. For example, arranging cells in a formation, and holding the pattern, or orchestrating pre-determined group behavior could all yield rich and unprecedented biological data.

CLINICAL: In addition to the high-resolution manufacturing of complex heterogeneous tissues, the closed-loop nature of the method could potentially eliminate product variability - another considerable bottleneck to delivering tissue-engineered products to clinical practice. Furthermore, serendipitously, the proposed approach also resolves product-size limitations[19] plaguing existing biomanufacturing techniques. Namely, the active vasculature of micro-channels can deliver nutrients and remove waste to/from any part of the tissue (unlike in current methods, where the cells die from lost access to the external medium). Finally, even if one could generate the perfect artificial tissue in a laboratory setting, training hospital staff to do the same on-site would mean teaching them custom culturing protocols for each new product. This is impractical, and is yet another critical commercialization hurdle resolved by this technology. Namely, automating the culturing configuration would allow companies to simply provide a computer code instead of a protocol. This would both simplify the process for the user, and ensure specification compliance specs are met in real-time.

FUTURE WORK: There are three key milestones for scaling up the 2D device to a 3D scaffold: 1) Design microfluidics plumbing for XYZ delivery / sampling (instead of just XY). 2) Fabricate the 3D scaffold; 3) Make it biodegradable. To that end, we will stack the 2D device architecture via CAD drawings, and then fabricate it in 3D using a digital micromirror device (DMD) for layer-by-layer photo crosslinking and ablation via a UV laser.[20] The final scaffold will be made from a *biodegradable* material (e.g., PLGA, PGS, Silk fibroin, APS or sugar).[6, 9, 21-23]

CONCLUSION

We have presented a microfluidic platform that can control the spatial delivery/sampling of chemical for manipulation of single-cell behavior in the XY plane. In the near future, we will extend this concept to XYZ manipulations within transparent, biocompatible and biodegradable 3D scaffolds. It is our hope that the technology will ultimately resolve the bottlenecks plaguing tissue engineering technologies today, and ultimately enable computer-driven tissue engineering through coupling with automation electronics. This would, in turn, allow machines to culture tissue reproducibly, and without the need to train hospital staff onsite.

The proposed technology would enable: 1) organ-sized engineered tissue via nutrient delivery and metabolic waste removal throughout the scaffold; 2) viable and consistent tissue products via orchestration of cell action during culturing; 3) improved cancer drug screening via noninvasive sampling of cell responses throughout the whole time course of administration; 4) biomanufacturing automation for achieving desired specifications on site, without the need to train hospital staff custom culturing protocols for every different tissue engineering product.

ACKNOWLEDGEMENTS

The authors also thank Gustavus and Louise Pfeiffer Research Foundation Major Investment Grant, New Jersey Health Foundation Research Award - Grant #PC 22-19, and NJIT Faculty Seed Grant for

their gracious funding of our work. Additionally, the authors would like to thank New Jersey Institute of Technology (NJIT)'s McNair Achievement and Provost Summer Research Programs for providing student labor for this project. Finally, we would like to thank Dr. Rafael Gómez-Sjöberg for providing us with software and blueprints for the addressable microfluidic technology published on his website.

COMPLIANCE WITH ETHICAL STANDARDS

Funding: This work was supported by the Gustavus and Louise Pfeiffer Research Foundation's Major Investment Grant, New Jersey Health Foundation Research Award - Grant #PC 22-19 and NJIT Faculty Seed Grant.

Competing Interests: The authors declare that a Provisional U.S. patent Application No. 62/753,622 filed on Oct 31, 2018.

Ethical approval: This article does not contain any studies with human participants or animals performed by any of the authors.

1. U. S. F. a. D. Administration, Approved Cellular and Gene Therapy Products, https://www.fda.gov/BiologicsBloodVaccines/CellularGeneTherapyProducts/ApprovedProducts/default.htm, (accessed 02/20/2018, 2018).
2. U. S. F. a. D. Administration, Approved Cellular and Gene Therapy Products, https://www.fda.gov/BiologicsBloodVaccines/CellularGeneTherapyProducts/ApprovedProducts/default.htm).
3. K. R. King, C. C. J. Wang, M. R. Kaazempur-Mofrad, J. P. Vacanti and J. T. Borenstein, *Advanced Materials*, 2004, **16**, 2007-2012.
4. C. J. Bettinger, E. J. Weinberg, K. M. Kulig, J. P. Vacanti, Y. Wang, J. T. Borenstein and R. Langer, *Advanced materials*, 2006, **18**, 165-169.
5. C. J. Bettinger, K. M. Cyr, A. Matsumoto, R. Langer, J. T. Borenstein and D. L. Kaplan, *Advanced Materials*, 2007, **19**, 2847-2850.
6. J. Wang, C. J. Bettinger, R. S. Langer and J. T. Borenstein, *Organogenesis*, 2010, **6**, 212-216.
7. J. S. Miller, K. R. Stevens, M. T. Yang, B. M. Baker, D.-H. T. Nguyen, D. M. Cohen, E. Toro, A. A. Chen, P. A. Galie and X. Yu, *Nature materials*, 2012, **11**, 768.
8. C. Cha, P. Soman, W. Zhu, M. Nikkhah, G. Camci-Unal, S. Chen and A. Khademhosseini, *Biomaterials science*, 2014, **2**, 703-709.
9. B. Zhang, M. Montgomery, A. Pahnke, L. Reis, S. S. Nunes and M. Radisic, 2013.
10. H.-Y. Wang, N. Bao and C. Lu, *Biosensors and Bioelectronics*, 2008, **24**, 613-617.
11. K. Leung, H. Zahn, T. Leaver, K. M. Konwar, N. W. Hanson, A. P. Pagé, C.-C. Lo, P. S. Chain, S. J. Hallam and C. L. Hansen, *Proceedings of the National Academy of Sciences*, 2012, **109**, 7665-7670.
12. Y. Gao, J. Tian, J. Wu, W. Cao, B. Zhou, R. Shen and W. Wen, *RSC Advances*, 2016, **6**, 101760-101769.
13. R. Gómez-Sjöberg, A. A. Leyrat, D. M. Pirone, C. S. Chen and S. R. Quake, *Analytical chemistry*, 2007, **79**, 8557-8563.
14. K. Brower, R. R. Puccinelli, C. J. Markin, T. C. Shimko, S. A. Longwell, B. Cruz, R. Gomez-Sjoberg and P. M. Fordyce, *HardwareX*, 2018, **3**, 117-134.
15. **R. Gómez-Sjöberg**, Rafael's Microfluidics Page, https://sites.google.com/site/rafaelsmicrofluidicspage/home).
16. Q. L. Pham, N. A. N. Tong, A. Mathew, S. Basuray and R. S. Voronov, *Biomicrofluidics*, 2018, **12**, 044119.
17. Q. L. Pham, L. N. Rodrigues, M. A. Maximov, V. D. Chandran, C. Bi, D. Chege, T. Dijamco, E. Stein, N. A. N. Tong, S. Basuray and R. S. Voronov, *Cellular and Molecular Bioengineering*, 2018, DOI: 10.1007/s12195-018-0551-x.
18. C. A. Schneider, W. S. Rasband and K. W. Eliceiri, *Nat Methods*, 2012, **9**, 671-675.
19. E. C. Novosel, C. Kleinhans and P. J. Kluger, *Advanced drug delivery reviews*, 2011, **63**, 300-311.
20. A. P. Zhang, X. Qu, P. Soman, K. C. Hribar, J. W. Lee, S. C. Chen and S. L. He, *Advanced Materials*, 2012, **24**, 4266-+.
21. D.-E. Mogosanu, R. Verplancke, P. Dubruel and J. Vanfleteren, *Materials & Design*, 2016, **89**, 1315-1324.
22. K. R. King, C. Wang, J. P. Vacanti and J. T. Borenstein, 2002.
23. J. T. Borenstein, K. Megley, K. Wall, E. M. Pritchard, D. Truong, D. L. Kaplan, S. L. Tao and I. M. Herman, *Materials*, 2010, **3**, 1833-1844.